EVOLUTION OF THE SOLAR WIND PLASMA PARAMETERS FLUCTUATIONS - ULYSSES OBSERVATIONS

NEDELIA ANTONIA POPESCU[1], EMIL POPESCU[2,1]

[1]*Astronomical Institute of Romanian Academy*
Str. Cutitul de Argint 5, 40557 Bucharest, Romania
Email: nedelia@aira.astro.ro
[2]*Technical University of Civil Engineering,*
Bd. Lacul Tei 124, 020396 Bucharest, Romania
Email: epopescu@utcb.ro

Abstract. The solar wind plasma parameters and interplanetary magnetic field fluctuations are studied for an interval of time that corresponds to Ulysses in-situ measurements of high-latitude heliospheric magnetic field, around the time of polarity reversal in 2001. Also the analyzed period in 2001 corresponds to the transition to the stationary fast flows, that starts from the day of the year (DOY) 240. Using data from Ulysses/ VHM instrument, the technique based on differencing of the original time series over a range of temporal scales have been considered for this study. The fluctuations of the magnetic field magnitude (B), and the corresponding RTN components (Br, Bt, Bn), at larger scales are less intermittent than at small scales. Their behaviour at different scales is quantitatively described by the probability distribution functions (PDFs) and generalized structure functions. Inside the studied interval of time, an ICME event can be observed between DOY 236.542 - DOY 237.042 of 2001, its signatures being also analyzed in this paper.

Key words: solar wind turbulence, solar wind plasma parameters fluctuations.

1. INTRODUCTION

Solar wind represents the continuous highly variable hot plasma that radially outflows from the Sun's corona, and moves at supersonic speeds, ranging from slightly below 300 km s^{-1} to about 2000 km s^{-1} during transient solar events. The magnetic field of the Sun, as well as different structures, waves and turbulent fluctuations on a wide range of scales are embedded within the solar wind.

The basic characteristic of the solar wind is represented by the two states of flow: fast streams and slow streams. These can be differentiated by kinetic parameters (speed, kinetic temperature), and more precisely by the elemental and charge state composition (see Feldman *et al.*, 2005). The compositional differences between the fast and slow solar wind appear because of their different origins in the corona.

From the first observations of the solar wind (Neugebauer and Snyder, 1962), it is known that the solar wind flows present variability on all timescales, that can be determined from the fluctuations of the solar wind plasma parameters and interplan-

etary magnetic field.

The intermittency in the solar wind is connected with the briskly occurrence, in space or time, of extreme events or large amplitude variations of plasma parameters, like the bulk velocity, or magnetic field magnitude.

In this paper we use statistical methods of analysis (probability distribution functions, and structure functions) for the investigation of solar wind plasma parameters and magnetic field intermittency.

We have to mention that the data provided by Ulysses for the year 2001 represent the first in-situ measurements of high-latitude heliospheric magnetic field around the time of polarity reversal. In 2001 around the DOY 236, at a heliolatitude of about 67° N, the last crossing of heliospheric current sheet was registered by Ulysses. Only the new northern polarity (inward polarity) was detected since that moment, with exceptionally short reversals during transient structures (Jones and Balogh, 2003).

Thus, the period studied in our work (between DOY 234 and DOY 238) represents a period of transition to the stationary fast flows (around 750 km s^{-1}), that starts from DOY 240 and lasts for a period of 100 days. For this long period only the high speed solar wind was observed at high heliolatitudes, Ulysses being positioned along the northern polar coronal hole.

Because 2000 - 2001 was a period of maximum solar activity, many extreme events were present such as transient ejections of solar material, the so-called coronal mass ejections (CMEs). Their interplanetary counterparts have been registered by Ulysses as interplanetary coronal mass ejections (ICMEs).

Such an ICME event can be observed between DOY 236.542 and 237.042 (Ebert *et al.*, 2009), its signatures being also analyzed in this paper. For our analysis we consider one-minute resolution data from VHM magnetometer instrument on board Ulysses spacecraft (for the magnetic field magnitude B), 4-minutes resolution data from SWOOPS/ Ulysses (for solar wind velocity V, density N, and temperature T), and 3 hour averaged data for temperature, plasma composition and charge-state measurements of solar wind ions from SWICS instrument. The analysis is realized for a period of 5 days, starting with the day of the year DOY 234 through DOY 238 of 2001.

In this paper we also present a detailed description and analysis of the ICME on 24 August 2001 by means of classical identification of ICMEs ($He++$ abundance enhancement, low kinetic temperature, low velocity); plasma dynamics signatures (thermal index $Ith > 1$); plasma composition signatures (anomalies of abundance and charge state of heavy ion species, low ion temperature and velocities).

2. SOLAR WIND PARAMETERS AND MAGNETIC FIELD DATA ANALYSIS

In this section we analyze the characteristics of the ICME event on DOY 236 (24 August 2001). During this event, Ulysses was situated above $67.5^{\circ}N$, and at the heliocentric distances 1.75 AU.

The duration of the ICME on 24 August 2001 is 12 hours: between 24 August at 13:00 UT (DOY 236.542), and 25 August at 01:00 UT (DOY 237.042). In order to analyze the characteristic signatures of an ICME we consider the in situ data recorded by Ulysses with SWOOPS, VHM and SWICS instruments. This ICME presents the features of a magnetic cloud: the magnetic field rotates smoothly through a large angle, the strength of the magnetic field is higher than in the average solar wind, and the temperature is lower than that in the average solar wind (Burlaga *et al.*, 1981; Burlaga, 1991). Within the event time frame an average magnetic field magnitude of $< B >= 8.42 \pm 1.45$ (nT) and proton velocity of $< V >= 539 \pm 9$ km s^{-1} of the plasma are determined (Ebert *et al.*, 2009).

2.1. CLASSICAL SIGNATURES AND PLASMA DYNAMICS SIGNATURE DETECTION OF ICME

Interplanetary magnetic field data obtained from the Ulysses spacecraft during the passage of the ICME are presented in Fig.1. The time is expressed in day of the year (DOY). The one minute resolution data obtained with VMH instrument are presented for an interval of 3 days, starting with DOY 235. From upper to lower panels are depicted: the components of the interplanetary magnetic field in RTN coordinates (Br, Bt, Bn), and the absolute value of the magnetic field B, as well as their corresponding normalized variances (*i.e.*, $\sigma^2/|B|^2$).

Also, the magnetic field components present a well defined large-scale feature, that can be recognized in the behaviour of the relevant normalized variances. The presence of the ICME corresponds to a sudden drop in the magnetic field variances in the interval delimited by the two vertical solid lines in Fig.1 (panels 2, 4, 6, and 8).

In Fig.2 are plotted from top to bottom, the proton number density Np, the alpha to proton number density ratio (*i.e.*, $N(He++)/N(H+)$ ratio), solar wind bulk velocity Vp, the ratio of proton temperature Tp and the expected temperature $Texp$ (determined with the formula of Lopez (1987)), for an interval of 3 days starting with DOY 235. The data are obtained by SWOOPS instrument, with a 4 minute resolution.

In Figs. 1 and 2 the vertical dashed line corresponds to the shock arrival on 24 August 2001, at 8:00 UT (*i.e.* DOY 236.33). The boundaries of the magnetic cloud are indicated by the first vertical solid line, that corresponds to the start of the field coherent rotation (the beginning of the MC on 24 August 2001, at 13:00 UT), and the second vertical solid line, that corresponds to the ending for the rotation of magnetic

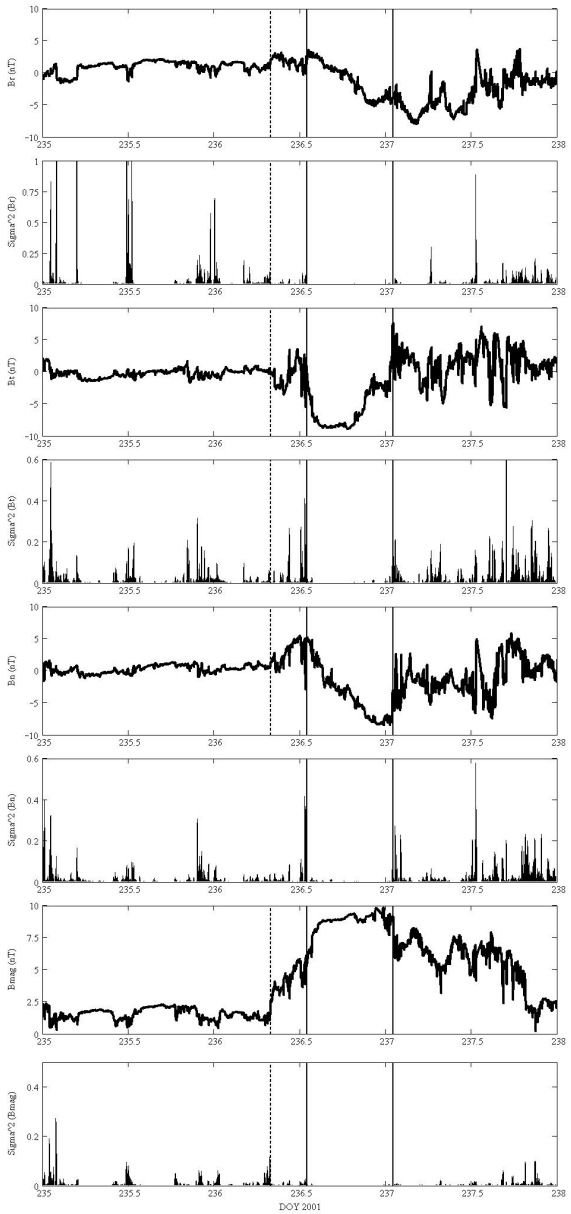

Fig. 1 – The magnetic field RTN components (Br, Bt, Bn), and magnetic field magnitude B, and the corresponding normalized variances for a time interval of 3 days.

field (end of the cloud on 25 August 2001, at 01:00 UT). In Fig. 2, the horizontal dashed line in the second panel, represents the 0.06 threshold (Hirshberg *et al.*, 1971;

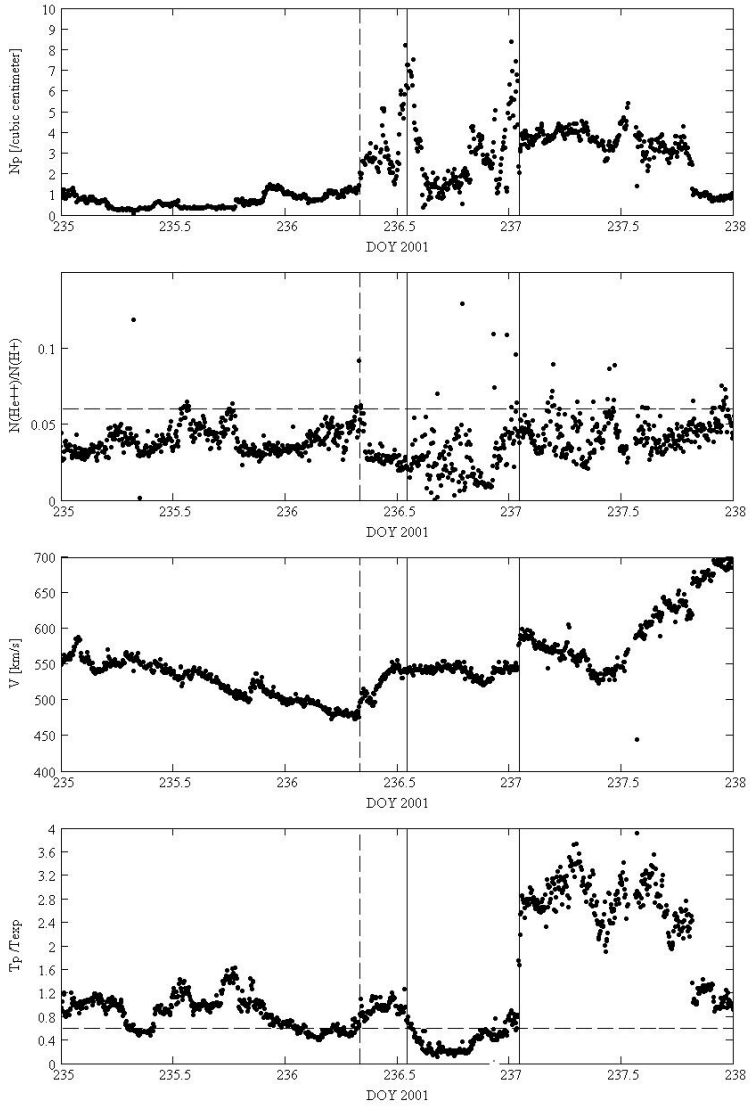

Fig. 2 – The proton number density Np, the alpha to proton number density ratio, solar wind bulk velocity Vp, and $Tp/Texp$, for a time interval of 3 days.

Borrini *et al.*, 1982) for the value of helium abundance.

Between the dashed line that corresponds to the shock arrival and the first solid vertical line, the sheath region is present. The arrival of a weak forward fast shock at Ulysses on DOY 236.33 can be observed in Fig. 1 and 2, this shock being identified in the data by the presence of discontinuities in the magnetic field intensity, proton

density, solar wind velocity, and proton temperature. These parameters present an increase at this time. During a time interval of 5 hours (between DOY 236.33 and DOY 236.542) the velocity is increasing from 475 km s^{-1} to 550 km s^{-1}. All these signatures indicate that immediately preceding the arrival of the MC, a hot, dense aggregation of the shocked sheath plasma is present.

The classical identification characteristics for an ICME can be observed in Figs. 1 and 2 during the interval between DOY 236.542 and DOY 237.042. The value of helium abundance (*i.e.* the alpha to proton number density ratio) is grater than 0.06 - 0.08. The criterion of abnormally low proton temperature (Tp) represents one of the primary ICME identification signatures. For the interval of the studied ICME, the proton temperature Tp follows the condition $Tp/Texp < 0.5$, where $Texp$ is calculated with the relations of Lopez (1987).

The condition stated by Richardson *et al.*(1997) regarding the proton (Tp) and electron (Te) temperatures (*i.e.*, $Te/Tp > 2$) is another indicator for the presence of an ICME. This condition is fulfilled by the studied event, according to Fig. 3 (top panel), that presents the comparison between the electron (steps) and proton (line) temperatures for a time interval of 3 days, starting with DOY 235.

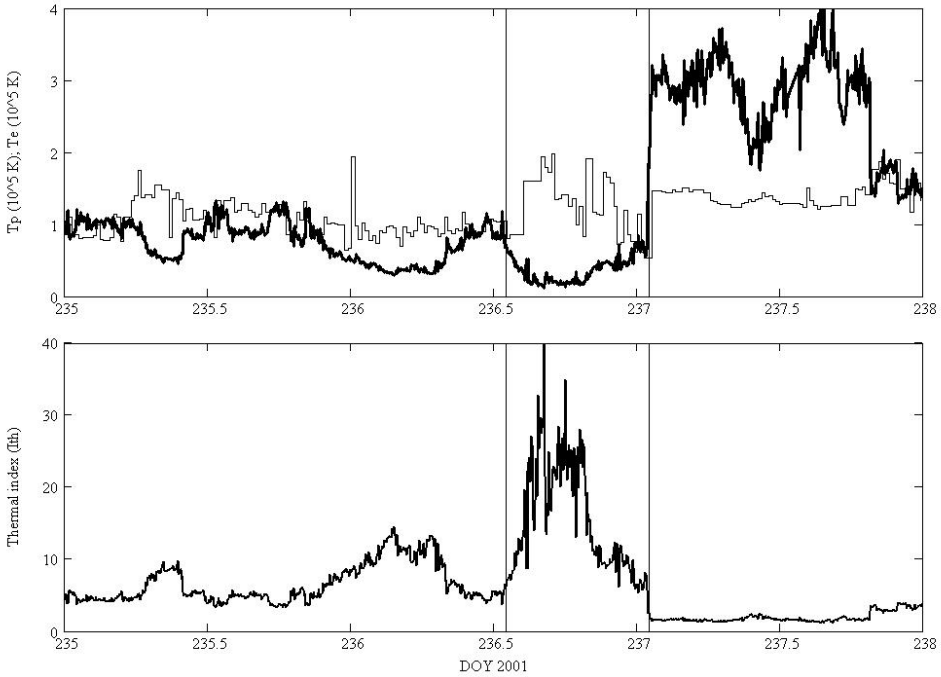

Fig. 3 – The comparison between the electron (steps) and proton (line) temperatures (top panel); the Ith thermal index (bottom panel), for a time interval of 3 days.

Plasma dynamics signature detection can be obtained using the *thermal index*, defined by Goldstein *et al.*(1998), as follows:

$$Ith = (500 \times Vp + 1.75 \times 10^5)/Tp \quad (1)$$

where Tp = plasma proton temperature; Vp = plasma proton velocity. If $Ith > 1$ plasma seems to be associated with an ICME (Goldstein *et al.*, 1998). Thermal index is a useful indicator because is mainly a result of the expansion of the plasma cloud as it propagates away from the sun.

In the case of the ICME registered on 24-25 August 2001, the thermal index riches very high values of about 35. The thermal index is displayed in Fig.3 (bottom panel), for a time interval of 3 days starting with DOY 235.

2.2. PLASMA COMPOSITION SIGNATURES ANALYSIS

For the plasma composition signatures detection, Popescu (2009) have used 3 hour averaged data for temperature, plasma composition and charge-state measurements of solar wind ions from SWICS instrument. This study is extended in this paper with new criteria of plasma composition signatures detection.

The present analysis underlines the following conclusions:

1) Criteria of low ion temperature is verified, in the studied interval of time all temperatures being low.

2) Heavy ion species present anomalies of abundance and charge state:

a) The optimum threshold value for the average Fe charge state is considered $< Q_{Fe} >= 11$ (Lepri and Zurbuchen, 2004). Greater values are indicators for the presence of ICMEs. The distributions of Fe average charge state and the Fe/O abundance are presented in Fig. 4 (top panel). In the studied interval of 5 days, the value of average iron charge state is between [10.5,11], and $Fe/O < 2$.

b) The enhanced charge-state ratios C(6+)/C(5+) and O(7+)/O(6+) can be observed in Fig. 4 (middle panel). Threshold O(7+)/O(6+) = 0.8 corresponds to a freezing-in temperature of 2.05×10^6 K, this condition being satisfied in the studied case. This result is in good agreement with the velocity distribution (in the studied interval of time the velocity is $\sim$ 550 km s^{-1}). In Fig.4 (middle panel) is also depicted with the continuous line the threshold established by Richardson and Cane (2004) for O(7+)/O(6+), in the case of an ICME:

$$O(7+)/O(6+) \geq 6.008 \times exp(-0.00578 \times Vp) \quad (2)$$

where Vp represents the solar wind bulk velocity.

For the 24 -25 August 2001 event, it is obvious that the charge-state ratios O(7+)/O(6+) is extremely high. Also, the charge-state ratios C(6+)/C(5+) is correlated with O(7+)/O(6+) ratio.

c) The enhancement of C(6+), Ne(8+), Mg(10+) densities relative to O(6+), can be observed in Fig.4 (bottom panel), for the quantities between the two vertical lines. Also, the criteria of Richardson and Cane (2004) have been also considered for Mg to O abundance ratio and Ne to O abundance ratio:

$$Mg/O > 0.982 \times exp(-0.00367 \times Vp) \tag{3}$$

$$Ne/O > 0.59 \times exp(-0.0017 \times Vp) \tag{4}$$

where Vp represents the solar wind bulk velocity.

Fig.4 (bottom panel) displays the Ulysses data for a 5 day interval, the upper dotted line representing the Ne/O abundance ratio obtained with the above formula, function of the solar wind speed. The lower continuous line represents the Mg to O abundance ratio determined with the formula of Richardson and Cane (2004). One observes that Mg/O is higher than this threshold, during the interval of the studied event. Only the condition for Mg/O is fulfilled in the case of the studied event.

The ICME registered on 24 - 25 August 2001 verifies almost all classical identification conditions, plasma dynamics and composition signatures. These signatures are not necessarily present simultaneously and define exact the same region of the solar wind. An enhanced helium abundance, depressed proton temperature, and smooth strong magnetic fields, compared with the ambient solar wind upstream of the shock, characterize this event.

3. STATISTICAL SCALING PROPERTIES OF INTERPLANETARY MAGNETIC FIELD TIME SERIES

In order to study the scaling and intermittency of the fluctuations for the magnetic field magnitude, B, and the RTN components (Br, Bt, Bn), we apply the finite size scaling technique on Ulysses data.

Intermittency refers to the statistical behaviour of the fluctuations in the spatial domain, but when the Taylor hypothesis is valid (*i.e.* a turbulent structure transits the space craft at a time which is small in comparison with its own evolution) time differences are equivalent to space differences.

In our study we consider the technique based on differencing of the original time series over a range of temporal scales τ. The fluctuations on temporal scale τ can be captured by a set of differences $dS(t,\tau) = S(t+\tau) - S(t)$, where $S(t)$ represents a given time series (Frisch, 1995).

First step in our calculation is represented by the determination of magnetic field magnitude differences, as well as for the RTN components Br, Bt, Bn, at a given scale $\tau_n = 2^n$ minutes ($n = 0, 1, 2, ..., 7$) through:

$$dB_n = dB_n(t_i, \tau_n) = [B(t_i + \tau_n) - B(t_i)] \tag{5}$$

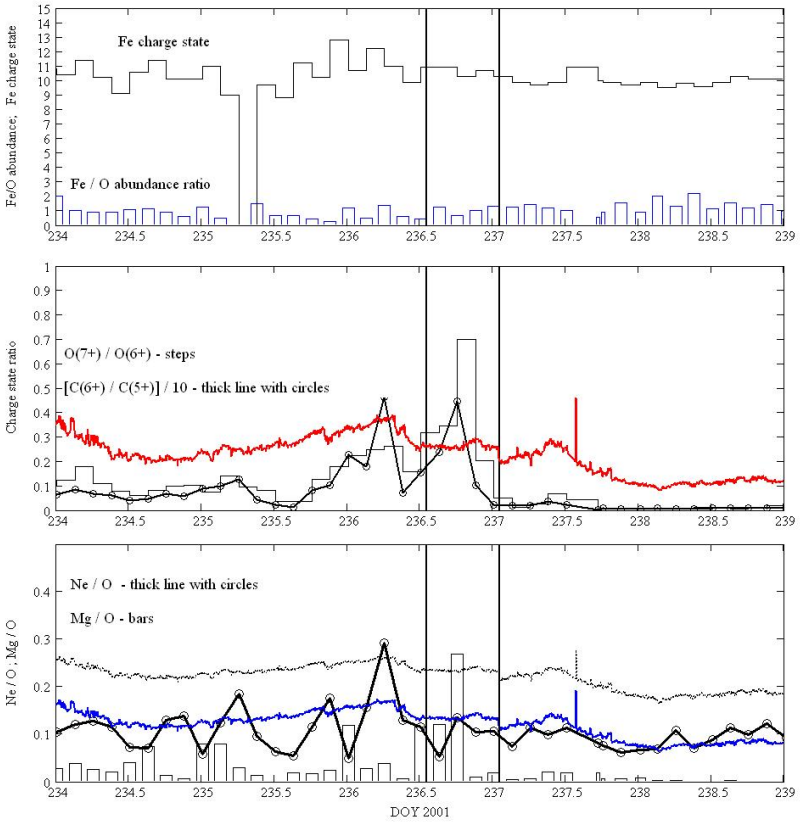

Fig. 4 – Fe average charge state and Fe/O abundance (top panel). Charge-state ratios C(6+)/C(5+) and O(7+)/O(6+) (middle panel). Ne(8+), Mg(10+) densities relative to O(6+)(bottom panel), for a time interval of 5 days, starting with DOY 234.

where t_i - the time (minutes); $B(t_i)$- the 1-minute resolution data for B, Br, Bt, Bn.

We considered scales ranging from $\tau_0 = 1$ minute to $\tau_7 = 2^7 = 128$ minutes ~ 2 hours, and obtained eight normalized data sets $dB_n(t_i, \tau_n)$, denoted $dB0$,...,$dB7$.

In Fig.5 the magnetic field magnitude differences $dB1$, $dB3$, $dB5$, $dB6$, $dB7$ for the magnetic field magnitude are plotted *versus* time (for a time interval of 3 days, starting with DOY 235).

3.1. PROBABILITY DISTRIBUTION FUNCTIONS

According to Marsch and Tu (1994), Sorriso-Valvo *et al.*(1999, 2001), both fast and slow solar wind streams are highly intermittent.

In the case of intermittent turbulent media, the probability distribution func-

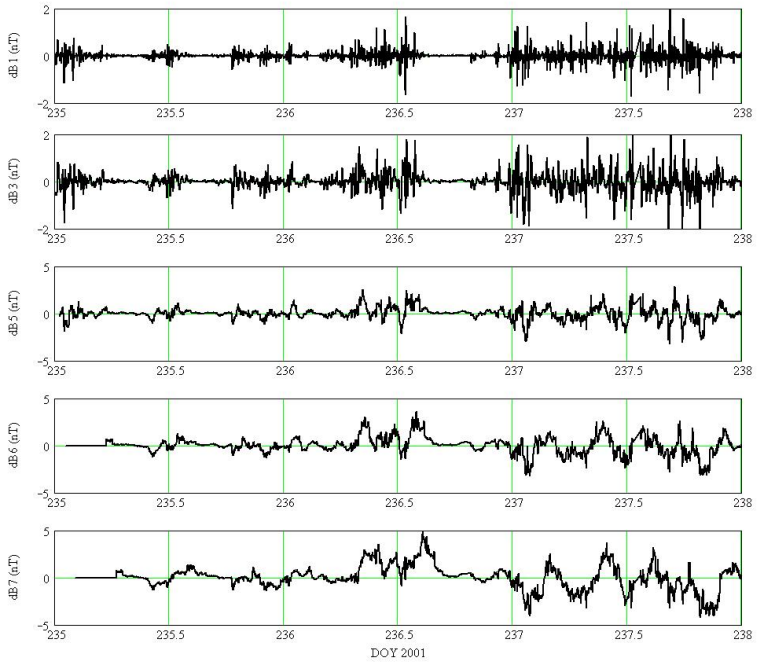

Fig. 5 – The magnetic field magnitude differences $dB1$, $dB3$, $dB5$, $dB6$, $dB7$ *versus* time, for a 3 days time interval.

tions (PDFs) of fluctuations have increasingly non-Gaussian shapes at smaller scales (Sorriso-Valvo *et al.*, 1999). Gaussian distributions for time lags longer than few hours fitt well the PDFs of the increments, while heavy-tailed shapes are present at scales smaller than few minutes. The fast streams are less intermittent than the slow wind flows, where the coherent structures are present and make the magnetic field fluctuations less random (Bruno *et al.*, 2003).

The properties of the intermittency of the magnetic turbulence in solar wind streams are strongly dependent on their regions of origin in the solar corona (Bruno *et al.*, 2003).

In Figs. 6, 7 and 8 are presented the unscaled PDFs of the magnetic field components dBr_n, dBt_n, dBn_n, respectively, for the considered time lags: $\tau_1 = 2$ minutes, $\tau_3 = 2^3 = 8$ minutes, $\tau_4 = 2^4 = 16$ minutes, $\tau_5 = 2^5 = 32$ minutes, $\tau_6 = 2^6 = 64$ minutes, and $\tau_7 = 2^7 = 128$ minutes. A time interval of 3 days, starting with DOY 235, is considered in our calculations. One observes at small scales the leptokurtic, long-tailed shapes of the PDFs. The values outside the core of the distribution especially rise from the major peaks of magnetic field fluctuations (see Popescu and Popescu, 2009).

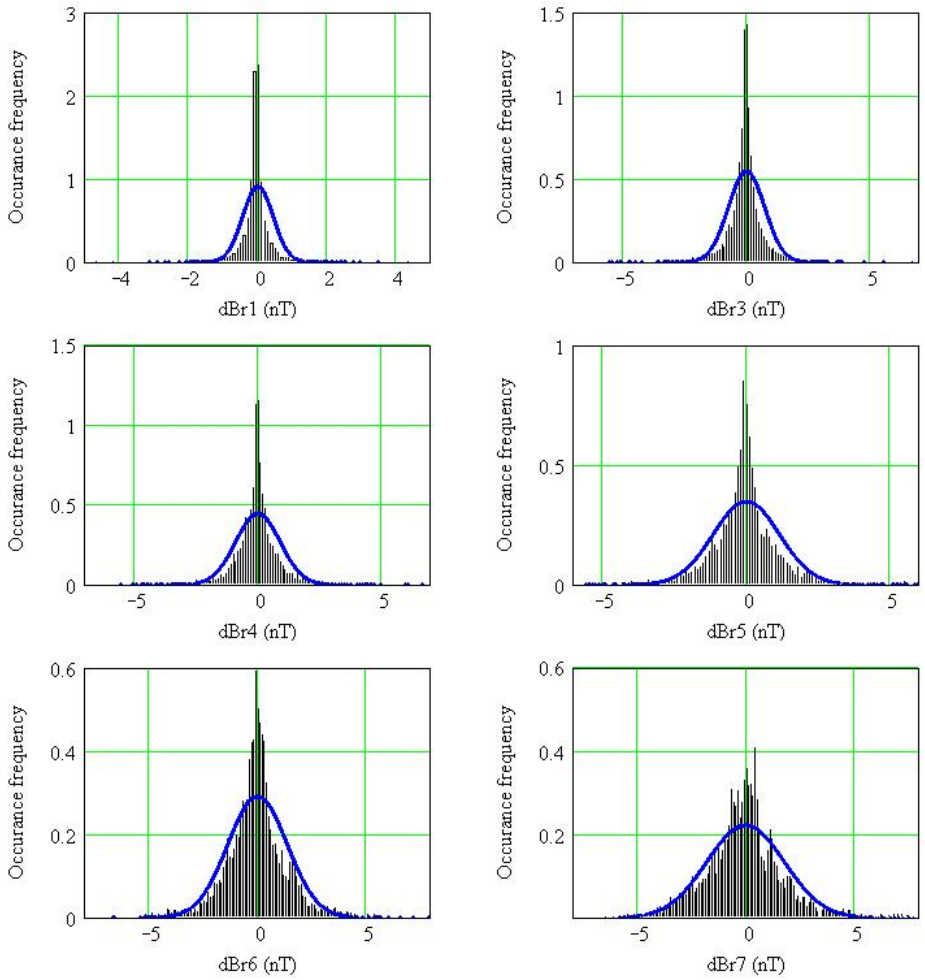

Fig. 6 – Unscaled PDFs for dBr_n, $n = 1, 3, 4, 5, 6, 7$ (bins of 0.1 nT are used for all lags).

3.2. GENERALIZED STRUCTURE FUNCTIONS ANALYSIS

We use high-order statistics to analyze the intermittent nature of the fluctuations. The generalized structure functions, particularly the third-order moment (skewness) and fourth-order moment (kurtosis), are important quantities to evaluate the degree of intermittency.

We have to mention that for Gaussian distribution the skewness and kurtosis equal zero, a positive (negative) skewness meaning a longer right (left) tail, and a positive (negative) kurtosis indicating a peaked (flat) distribution. A distribution with positive (negative) kurtosis is called leptokurtic (platykurtic).

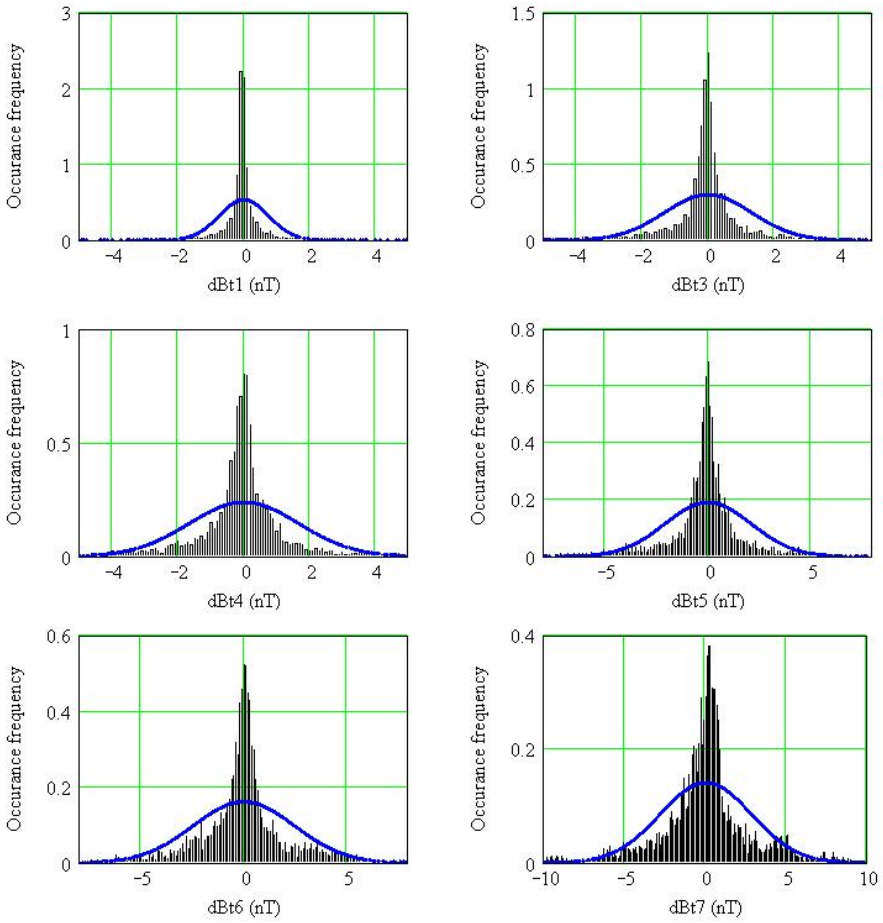

Fig. 7 – Unscaled PDFs for dBt_n, $n = 1, 3, 4, 5, 6, 7$ (bins of 0.1 nT are used for all lags).

The standard deviation, skewness, and kurtosis are plotted in Fig. 9 for the PDFs of the differences $dB_n(\tau_n)$, $dBr_n(\tau_n)$, $dBt_n(\tau_n)$, and $dBn_n(\tau_n)$, as a function of scale $n = log_2(\tau)$.

For the magnetic field magnitude and magnetic field components we can see a similar behaviour at all scales for the standard deviation and kurtosis (Fig.9 top and bottom panels).

As can be observed from Fig.9 (top panel) the standard deviation has an increasing trend with the increasing scale, with values between 1.2 nT and almost 3 nT, for $\tau_7 = 128$ minutes.

The kurtosis of $dB_n(\tau_n)$ and the other three magnetic field components differences is decreasing with increasing scale, at small scale a large kurtosis being

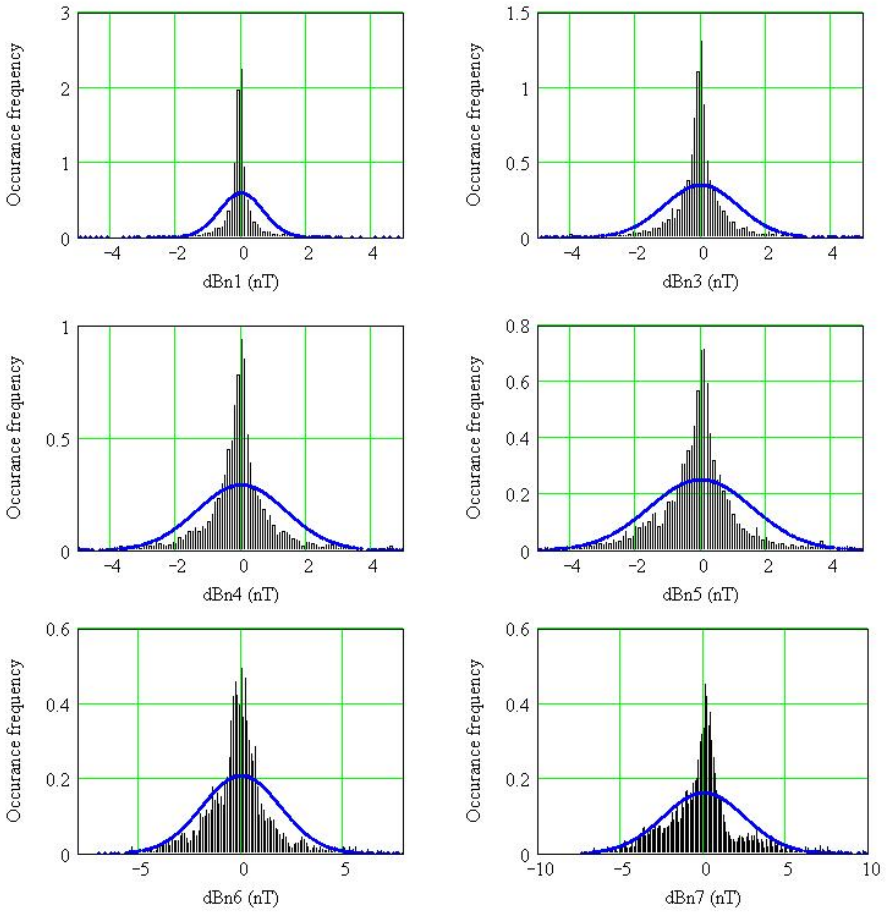

Fig. 8 – Unscaled PDFs for dBn_n, $n = 1, 3, 4, 5, 6, 7$ (bins of 0.1 nT are used for all lags).

associated with intermittent turbulence. The leptokurtic characteristics of PDFs for magnetic field fluctuations can be observed in Fig. 9 (bottom panel).

For $dBr_n(\tau_n)$, skewness presents negative values at small scales, its general values being in the interval [-2,0.5]. For $dB_n(\tau_n)$, $dBt_n(\tau_n)$, and $dBn_n(\tau_n)$, the skewness has mainly positive values, consistent with the shape of the distributions presented in Figs. 6, 7, and 8.

4. CONCLUSIONS

Multi-scale statistical methods such as PDFs analysis, and generalized structure functions have been considered for the study of interplanetary magnetic field

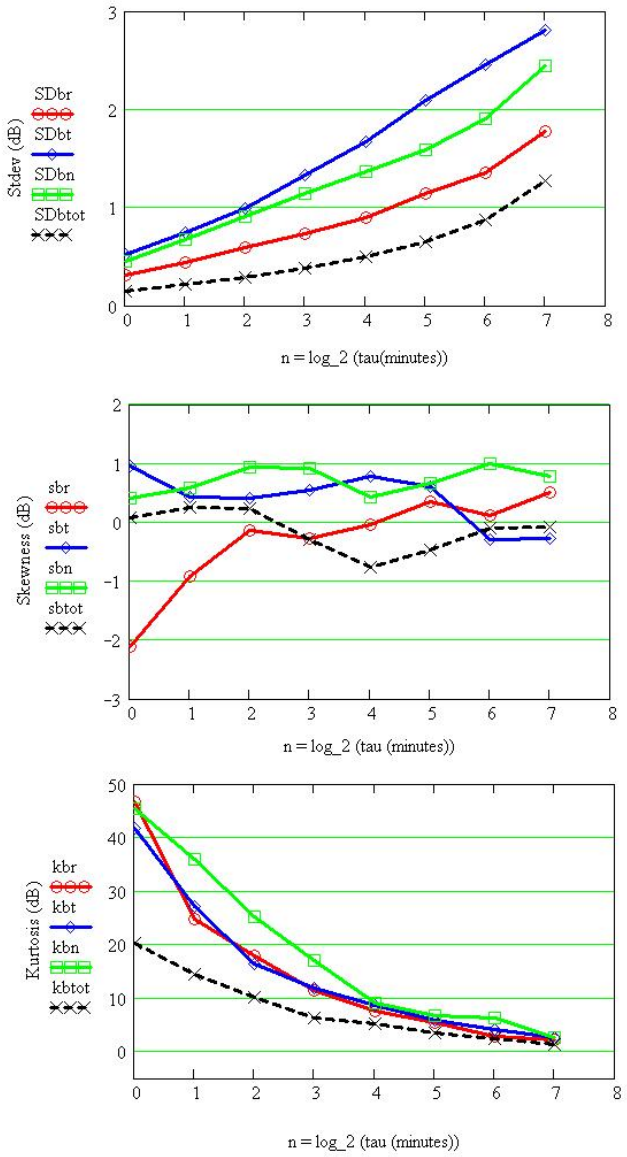

Fig. 9 – The high-order moments of dB_n, dBr_n, dBt_n, dBn_n as function of scale $n = log_2(\tau)$.

fluctuations, for the interval between DOY 235 - DOY 238, using data for the year 2001 from Ulysses/VHM instrument.

The fluctuations of the magnetic field magnitude (B), and the corresponding

RTN components (Br, Bt, Bn), at larger scales are less intermittent than at small scales. Their behaviour at different scales is quantitatively described by the probability distribution functions (PDFs) and generalized structure functions.

The values outside the core of the distribution especially rise from the major peaks of magnetic field fluctuations, caused mainly by the presence of the transient event on 24 - 25 August 2001 (DOY 236.542 - DOY 237.042). These values are mostly present at larger scales, $\tau_6 = 2^6 = 64$ minutes ~ 1 hour, and $\tau_7 = 2^7 = 128$ minutes ~ 2 hours, for Bt and Bn components of magnetic field. The analysis of the PDFs of the magnetic field increments revealed that the fourth-order moment of the distributions (*i.e.*, the kurtosis) increases as the time lag decreases.

The signatures of the ICME event that can be observed between DOY 236.542 - DOY 237.042 have been also analyzed. Almost all classical identification conditions, plasma dynamics and composition signatures have been verified by this ICME, that presents evident features of a magnetic cloud.

REFERENCES

Borrini, G., Gosling, J.T., Bame, S.J., and Feldman, W.C.: 1982, *J. Geophys. Res.* **87**, 7370.
Bruno, R., Carbone, V., Sorriso-Valvo, L., and Bavassano, B.: 2003, *J.Geophys. Res.* **108**, 1130.
Burlaga, L., Sittler, E., Mariani, F., and Schwenn, R.: 1981, *J. Geophys. Res.* **86**, 6673.
Burlaga, L.F.E.: 1991, *Physics of the Inner Heliosphere II*, 1.
Ebert, R.W., McComas, D.J., Elliott, H.A., Forsyth, R.J., and Gosling, J.T.: 2009, *J.Geophys. Res. A* **114**, 1109.
Feldman, U., Landi, E., and Schwadron, N.A.: 2005, *J.Geophys. Res.* **110**, 7109.
Frisch, U.: 1995, *Turbulence. The legacy of A. N. Kolmogorov., by Frisch, U.. Cambridge University Press, Cambridge (UK), 1995, XIII + 296 p., ISBN 0-521-45103-5.*
Goldstein, R., Neugebauer, M., and Clay, D.: 1998, *J. Geophys. Res.* **103**, 4761.
Hirshberg, J., Asbridge, J.R., and Robbins, D.E.: 1971, *Solar Phys.* **18**, 313.
Jones, G.H. and Balogh, A.: 2003, *Ann. Geophys.* **21**, 1377.
Lepri, S.T. and Zurbuchen, T.H.: 2004, *J.Geophys. Res. A* **109**, 6101.
Lopez, R.E.: 1987, *J. Geophys. Res.* **92**, 11189.
Marsch, E. and Tu, C.Y.: 1994, *Annales Geophysicae* **12**, 1127.
Neugebauer, M. and Snyder, C.W.: 1962, *Science* **138**, 1095.
Popescu, N.A. and Popescu, E.: 2009, *Romanian Astron. J.* **19**, 119.
Popescu, N.A.: 2009, *IAU Symposium* **257**, 295.
Richardson, I.G., Farrugia, C.J., and Cane, H.V.: 1997, *J. Geophys. Res.* **102**, 4691.
Richardson, I.G. and Cane, H.V.: 2004, *J.Geophys. Res.* **109**, 9104.
Sorriso-Valvo, L., Carbone, V., Veltri, P., Consolini, G., and Bruno, R.: 1999, *Geophys. Res. Lett.* **26**, 1801.
Sorriso-Valvo, L., Carbone, V., Giuliani, P., Veltri, P., Bruno, R., Antoni, V., and Martines, E.: 2001, *Planetary and Space Science* **49**, 1193.

Received on 5 October 2012